Post-liquefaction behavior determined by in-situ investigations after earthquakes

Hiroshi Nakazawa
National Research Institute for Earth Science and Disaster Resilience, Tsukuba, Japan, nakazawa@bosai.go.jp

Tadashi Hara
Koch University, Kochi, Japan, haratd@kochi-u.ac.jp

Daisuke Suetsugu
Miyazaki University, Miyazaki, Japan, suetsugu@cc.miyazaki-u.ac.jp

Masashi Kitazawa
Daiichi-Consultants Co., Ltd., Kochi, Japan, m-kitazawa@daiichi-c.co.jp

ABSTRACT: Generally, an increase in excess pore water pressure in a liquefied sand layer leads to a simultaneous loss of in-situ strength. Then, after such a transitional change of soil characteristics in the liquefied layer, it is thought that its undrained shear strength will recover to the original strength before liquefaction, as excess pore water pressure is dissipated. However, some reports based on observations after liquefaction indicated that the recovery of undrained shear strength occurred gradually over a long period. According to ground damage caused by liquefaction during past earthquakes, in-situ comparison of *N*-values by standard penetration tests before and after the event at liquefied sites mostly showed that *N*-values after an earthquake did not necessarily recover to their original states. However, although the process of liquefaction is generally considered by numerical analysis and laboratory tests, like undrained cyclic shear tests and model tests, this post-liquefaction behavior can seldom be seen in the field, especially when the focus is on estimation of in-situ characteristics. Estimation of post-liquefaction behavior, as well as the process leading to liquefaction, is important for developing earthquake-resistant design methods and countermeasures against liquefaction. This paper describes observational results of post-liquefaction behavior after the 2016 Kumamoto Earthquake. After this earthquake, a series of portable dynamic cone penetration tests was conducted periodically at the liquefied site for about 3 years. This testing revealed that the cone penetration resistance at the same depth remained low just after liquefaction. However, it seems that cone penetration resistance increased to more than the value before the earthquake after dissipation of excess pore water pressure.

Keywords: liquefaction; post-liquefaction behavior; excess pore water pressure; cone penetration resistance; in-situ investigation

1. Introduction

Generally, when a large earthquake occurs, an increase in excess pore water pressure due to liquefaction in loose sand leads to a simultaneous decrease in the undrained shear strength and shear modulus. Then, as shown in Fig. 1, it is thought that liquefied sand recovers to the state that existed before the earthquake as excess pore water pressure dissipates and the liquefied soil layer densifies. These recovery tendencies are considered to depend on various factors, such as deposition conditions in the liquefied soil layer, relative density, effective overburden pressure, amount of excess pore water pressure and its drainage conditions, and the initial conditions that lead to liquefaction susceptibility.

On the other hand, in cases of ground damage due to liquefaction by past earthquakes, as determined by comparison of *N*-values obtained from standard penetration tests before and after the event at liquefied sites, it was recognized that *N*-values after an earthquake do not necessarily recover to their original states. However, although the process of liquefaction is generally considered by numerical analysis and in laboratory tests, such as undrained cyclic shear and model tests, in-situ observation of post-liquefaction behavior is seldom performed. Estimation of the post-liquefaction behavior, as well as the process to liquefaction, is important for earthquake-resistant designs and countermeasures against liquefaction.

In a previous study, to investigate post-liquefied soil characteristics, the *N*-values before and after liquefaction were estimated based on the results of investigations at several sites liquefied by the 1995 Hyogo-ken Nanbu Earthquake, the 2000 Tottori-ken Seibu Earthquake, and the 2011 Great Tohoku Earthquake, as well as a full-scale field experiment by using the controlled blast technique. Additionally, the Kumamoto Earthquake occurred in April 2016 and caused serious damage due to liquefaction in residential areas in Kumamoto City, Kyushu Island, Japan. After this earthquake, a series of light-weight portable dynamic cone penetration tests was conducted periodically at the liquefied site for about 3 years. This paper mainly describes the recovery process of liquefied soil layers based on in-situ investigation results.

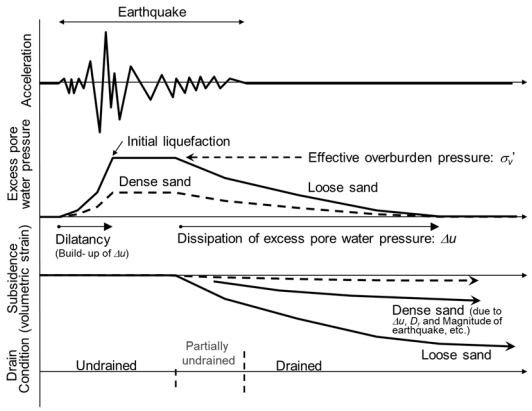

Figure 1. Typical in-situ behavior of soil layer liquefied by an earthquake.

2. Previous on-site investigations of post-liquefaction soil

The targets of past earthquakes and locations of the investigation sites in this paper are shown in Fig. 2. The results of previous studies at three of these sites are summarized in Figs. 3-5. These figures show the comparisons of *N*-values obtained from standard penetration tests or Swedish weight sounding tests (SWSTs) carried out before and after three earthquakes. Additionally, based on these results, safety factors against liquefaction, F_L, were calculated for each *N*-value distribution and shown in Figs. 3-5 along with the *N*-value distribution. To estimate liquefaction susceptibility, F_L was calculated according to the conditions [1-5] shown in Table 1 based on Japanese highway bridge specifications [6]. At each site, the calculation considered the same maximum ground surface acceleration and affected stratum as in the earthquake.

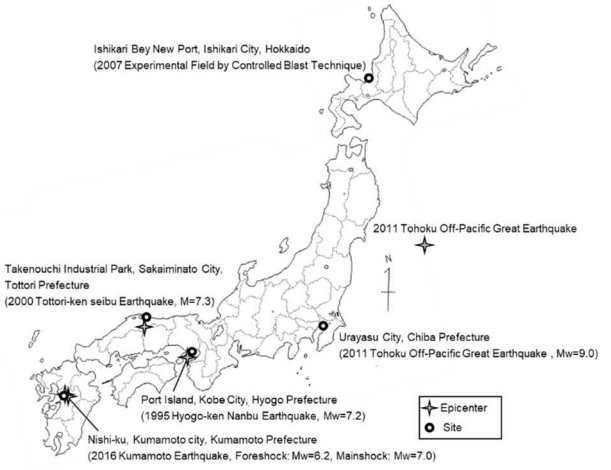

Figure 2. Location of study sites.

Table 1. List of evaluation conditions for F_L

Earthquake	Max. Acceleration (Gal)	Seismic motion type	Reference No.
1995 Hyogo - ken Nanbu Earthquake	341 Gal	Inland	
2000 Tottori-Ken Seibu Earthquake	302 Gal	Inland	
2011 off the Pacific coast of Tohoku Earthquake	200 Gal	Plate boundary	
Controlled Blast Technique	200 Gal	(Plate boundary)	[2]
2016 Kumamoto Earthquake	Level2 (K_h=0.6)	Inland	

2.1. Post-earthquake liquefaction behavior based on on-site investigation

It is well known that gravel deposits in reclaimed land were heavily liquefied during the 1995 Hyogo-ken Nanbu earthquake. Kobe City [7] reported the investigation results for the seismic array observation site on Port Island before and after the earthquake. In the investigation about 5 months after the earthquake, as shown in Fig. 3, it is difficult to grasp the process of *N*-value changes after liquefaction from the *N*-values before the earthquake.

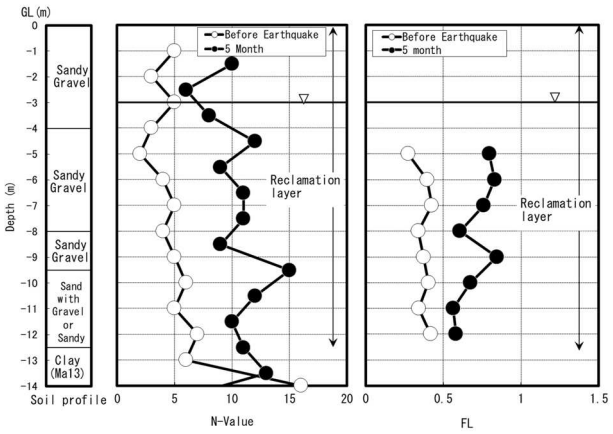

(a) *N*-value (b) Liquefaction safety factor

Figure 3. Comparison before and after the 1995 Hyogo-ken Nanbu Earthquake [7].

In the 2000 Tottori-ken Seibu Earthquake, liquefaction occurred over a wide area. Especially in the Takenouchi Industrial Park, liquefaction in a reclaimed layer of dredged non-plastic silt was confirmed [8]. In this site, Yamamoto et al. [9] conducted SWSTs at 1 and 12 days, and the recovery of *N*-values estimated from N_{sw} in the liquefied silt layer was reported. *N*-values obtained 2 years after the earthquake by Nakazawa et al. [10] are also shown in Fig. 4(a).

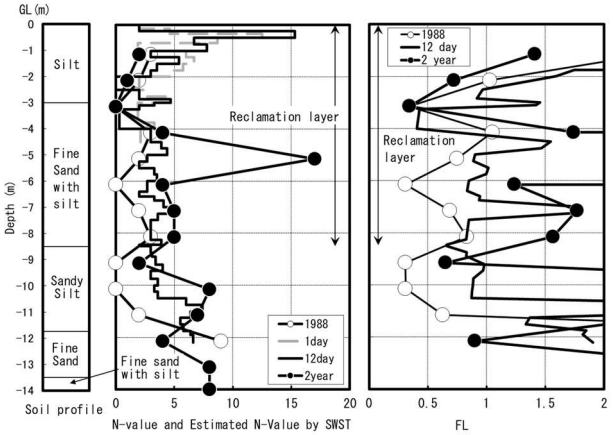

(a) *N*-value (b) Liquefaction safety factor

Figure 4. Comparison before and after the 2000 Tottori-ken Seibu Earthquake [9, 10].

Moreover, large-scale ground damage due to liquefaction in the Kanto Plain occurred in the 2011 Great Tohoku Earthquake. Especially, it is well known that liquefaction of housing sites on reclaimed land and differential subsidence of numerous houses was confirmed in Urayasu City. Ishii et al. [11] periodically conducted

SWSTs 1 and 6 months after this earthquake to estimate the liquefied characteristics at four points in a housing site and described the long-term recovery tendency of liquefied soil layer by comparing the distribution of N_{sw} obtained by SWST. Fig. 5(a) shows typical data indicating the recovery tendency of properties in a liquefied layer. The F_L distribution in Fig. 5(b) was obtained based on estimated N-values calculated from SWSTs performed by Inada [12].

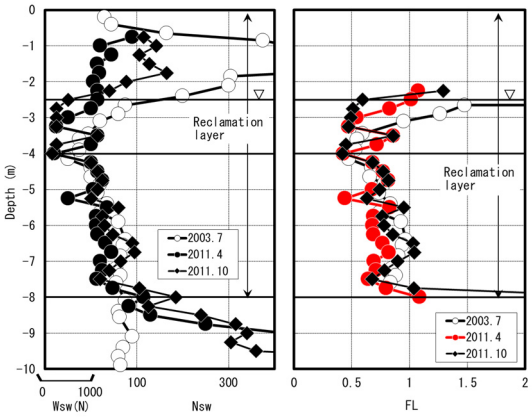

(a) N-value (b) Liquefaction safety factor

Figure 5. Comparison before and after the 2011 Great Tohoku Earthquake [11].

2.2. Post-liquefaction behavior measured by controlled blast technique

To observe actual damage to airport facilities caused by liquefaction and related phenomena, a full-scale liquefaction experiment employing the controlled blast technique was carried out as a preliminary experiment at Soma Port and then at Ishikari Bay New Port in Hokkaido Island, Japan, in October 2007. In this experiment by Nakazawa et al., the liquefaction process was studied by estimating in detail the dissipation of excess pore water pressure after blasting and the liquefied ground state 2 years after the experiment [5].

Fig. 6 indicates the N-value distribution at Soma Port. Though blasting was carried out at a depth of 4 m below ground level (GL-4m) and GL-8m in Fs1 and Fs2 layers equivalent to reclaimed deposits, no significant change in N-value distribution occurred 113 days after blasting.

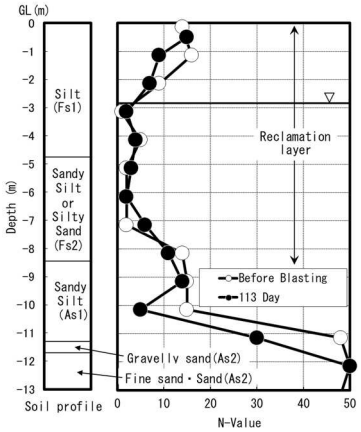

Figure 6. Comparison before and after the experiment at Soma Port [5].

Fig. 7 shows the results obtained from mini-ram sounding. This test is a simple method to acquire data related to the N-values by driving a rod equipped with a cone which top angle is 90 degrees and 36.6 mm in diameter with a 30 kg hammer from a height of 350 mm automatically. Blow counts, N_m, is usually measured every 20 cm. Finally, the N-values are calculated as half of N_m.

According to this figure, the N-value distribution decreased slightly 1 hour after blasting because of remarkable liquefaction from blasting, and recovery of N-values was recognized after 1 day, when excess pore water pressure dissipated completely. The recovery tendency of the blasting layer can be confirmed more clearly in the F_L distribution.

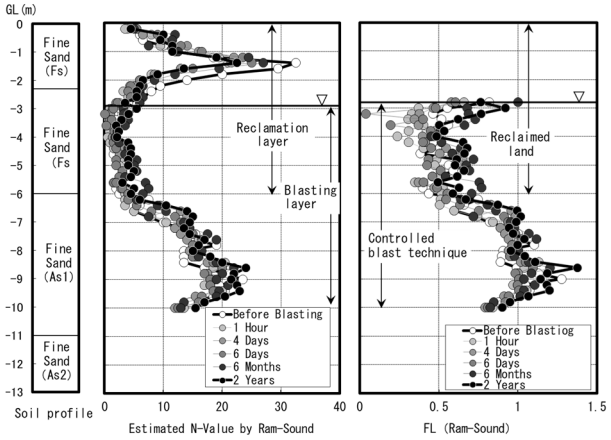

(a) N-value (b) Liquefaction safety factor

Figure 7. Comparison before and after experiment at Ishikari Bay New Port [5].

2.3. Change in liquefaction strength after earthquake

Generally, liquefaction strength is known to depend largely on relative density, D_r, and fine content, F_c, of a specimen, but a change in D_r is considered to be dominant in the dissipation of excess pore water pressure after liquefaction. Figures 8 and 9 compare the increase rate of liquefaction strength for various undisturbed reclaimed layers and natural deposits with respect to liquefaction strength before an earthquake or blasting. Liquefaction strength, R_L, is defined as $\sigma_d/2\sigma_c'$ at 5% of the double amplitude, DA, after 20 cycles, N_c, obtained from undrained cyclic tri-axial tests. As discussed previously, a change in liquefaction strength is considered to be different depending on factors such as the timing of the laboratory test and physical properties such as F_c. Regarding the results for the Soma and Ishikari sites, these data were obtained after sufficient time had passed since liquefaction.

As shown in Fig. 9, it is difficult to confirm the tendency of the increase rate in liquefaction strength with respect to F_c. However, after a certain amount of time passes, it can be seen that rate exceeds 1.0, and R_L becomes larger than the original liquefaction strength in Fig. 8.

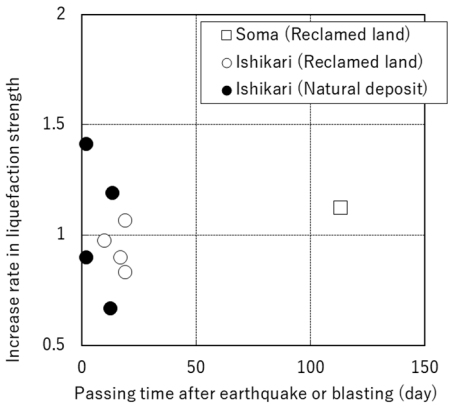

Figure 8. Increase rate in R_L after passage of time.

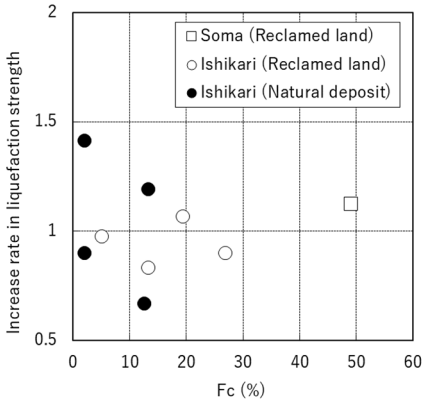

Figure 9. Relationship between F_c and increase rate in R_L.

2.4. Laboratory model test on change of S-wave velocity in liquefied sandy soil

The results of continuous measurement of changes in S-wave velocity, V_s, after artificial cyclic shearing to liquefy model ground were reported by Kusunoki et al. [13]. In this model test, the model ground was prepared by the air pluviation method with Soma No. 5 silica sand (F_c=0%; mean particle diameter, D_{50}=0.353 mm; and coefficient of uniformity, U_c=1.6) in a small rigid soil container measuring 545 mm in width, 461.5 mm in length, and 708.4 mm in height. The final D_r value over the whole model ground was 33% on average. After this model ground was liquefied, a small impact was applied to the bottom of the soil container with a wooden hammer to generate S waves in the model. V_s was obtained by reading the rise time of the traveling waveform with an accelerometer installed on the ground surface. This measurement was performed regularly over a long period of about 5 months.

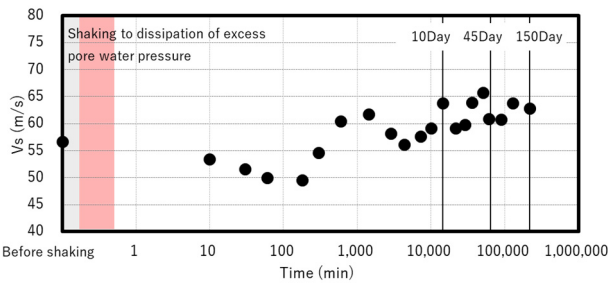

Figure 10. Recovery process of S-wave velocity in testing of liquefied sand model [13].

Figure 10 shows the change of V_s during the observation period after liquefaction. It is confirmed that V_s decreased until 100 min after dissipation of excess pore water pressure and became lower than the initial value before liquefaction. After that, V_s gradually showed a recovery trend and attained a larger value than the initial value before liquefaction.

3. On-site liquefaction investigations after the 2016 Kumamoto Earthquake

The Kumamoto Earthquake was preceded by a foreshock (M_W = 6.2) that occurred at 21:26 on April 14, and the main shock (M_w = 7.0) occurred at 1:25 on April 16, 2016. In Mashiki Town, Nishihara Village, and Minami Aso Village near the fault, it was reported that remarkable damage was caused by slope failure and collapse of residential housing due to strong motion [14]. In addition to this damage, other areas in Kumamoto City and Mashiki Town classified as fine terrain, such as flood plains, old river channels, and natural dikes, became extensively liquefied. Especially, subsidence and tilting of 2-story wooden houses in residential areas were severe, and Fig. 11 shows how a pile-supported foundation was exposed by settlement around houses due to liquefaction. Such issues threaten the life safety.

Figure 11. Exposure of pile-supported foundation due to liquefaction.

3.1. Features of investigation site obtained during previous study

A total of five on-site liquefaction investigations were conducted on May 5, 2016; July 26, 2016; January 21, 2017; June 9, 2017; and August 16, 2019, at Juso Child Park (Fig. 12). On May 5, 2016, Hara et al. investigated the site and provided an overview of the liquefied ground [15]. The liquefaction characteristics of the investigation site are described below with reference to the previous results shown in Fig. 13.

Figure 12. Investigation site in Kumamoto City [10].

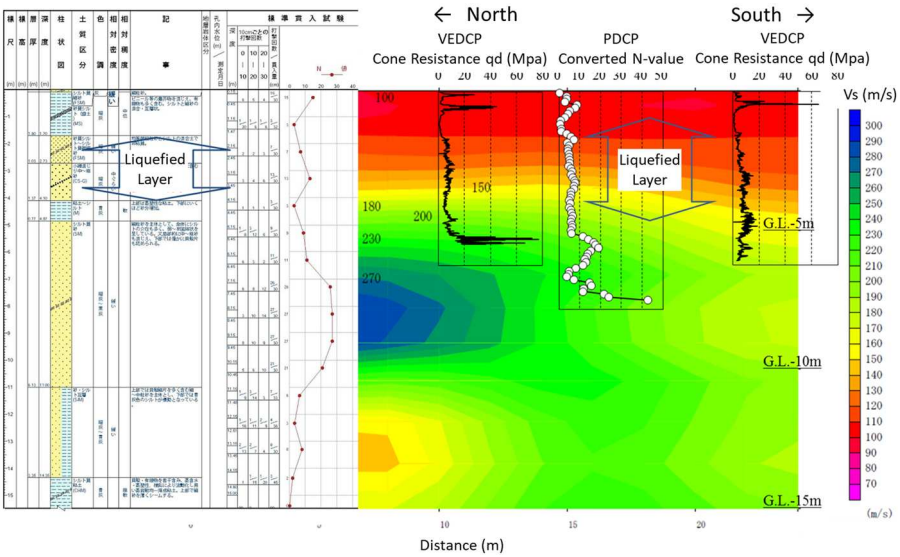

Figure 13. Summary of ground investigation results from a previous study [15].

In the previous study, surface wave exploration and sounding tests were conducted. Among these, the results of a portable dynamic cone penetration test show that a loose layer had an *N*-value converted to less than 10 and this low *N*-value distribution continued near GL-5m, below the groundwater surface of GL-1m. Moreover, it was confirmed that the post-liquefaction *N*-value distribution increased deeper than GL-5m.

Additionally, according to the results of surface wave exploration, a soil layer with a low S-wave velocity equivalent to 100 m/s existed from the surface down to GL-2m, and the V_s distribution was about 200 m/s deeper than GL-5m. The boring log [16] displayed on the left side of the same figure shows the results obtained before the earthquake at Akita-Higashi Elementary School, located about 50 m north of the investigation site (Fig. 12). Hara et al. [15] reported that the main strata where liquefaction occurred consisted of fine sand deposits from GL-1 to -5m.

3.2. Sounding test used in this study

The survey method typically used in this study was the Variable Energy Dynamic Cone Penetrometer (VEDCP), also called as PANDA, as shown in Fig. 14. The locations of test points were No. 1 at distance of 10 m from the starting point and No. 2 at 28.5 m along the surface wave exploration line shown in Figs. 12 and 13.

VEDCP is sounding equipment developed in France, and it has been widely used for evaluation of compacted ground, such as embankments. However, the applicability to natural sediments is unknown because there are few examples of this implementation. The results obtained from VEDCP were the dynamic penetration resistance values represented as q_d (MPa). Therefore, to evaluate the state of the liquefied layer as an *N*-value, correlation with the mini-ram sounding conducted separately at position No. 1 was obtained on July 26, 2016, and the q_d values at this site were converted to *N*-values with Eq. (1), as proposed by Nakazawa et al. [4].

$$N=0.6q_d \quad (1)$$

VEDCP is described below. Figure 15 presents a schematic diagram of a VEDCP test, and Fig. 16 shows its apparatus [17].

Figure 14. Variable Energy Dynamic Cone Penetrometer.

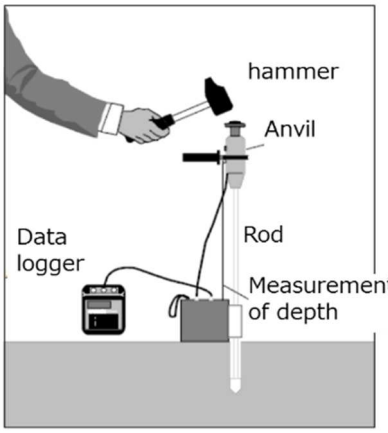

Figure 15. Schematic diagram of a cone penetration test with Variable Energy Dynamic Cone Penetrometer. [17].

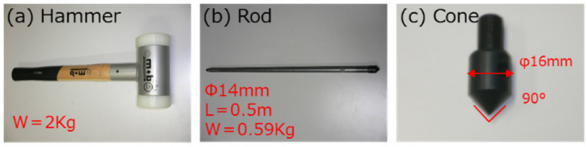

Figure 16. VEDCP apparatus: (a) hammer, (b) extension rod, and (c) cone.

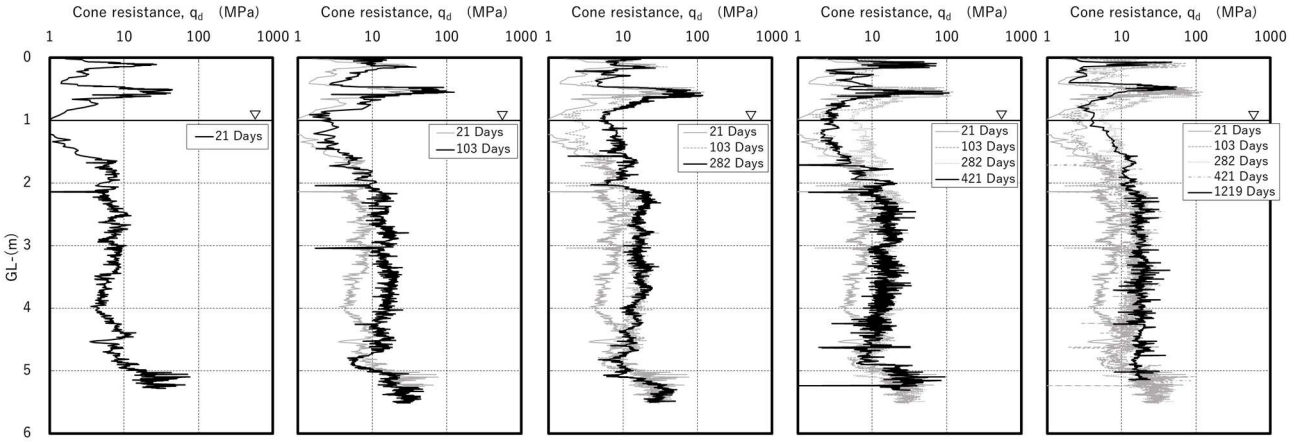

(a) May 5, 2016 (b) July 26, 2016 (c) January 21, 2017 (d) June 9, 2017 (e) August 16, 2019

Figure 17. Results obtained from variable energy dynamic cone penetrometer.

In a VEDCP test, extension rods with a cone having a diameter of 16 mm and tip angle of 90° are driven into the soil by a 2 kg-hammer blow with any energy input. For each hammer blow, VEDCP provides the depth of cone penetration and the speed of impact, yielding q_d at each depth increment. VEDCP can be operated by one man in a small space, and variable energy can be used for cone penetration. It needs only a short period for test time, and it shows the results immediately after the test. The depth of cone penetration is measured by a retractable tape, and the speed of impact is acquired by accelerometers in the anvil. The q_d is calculated as

$$q_d = \frac{1}{A}\frac{\frac{1}{2}MV^2}{1+\frac{P}{M}}\frac{1}{x}, \qquad (2)$$

where A is the area of the cone, M is the weight of the striking mass, P is the weight of the struck mass, V is the speed of impact, and x is the depth of cone penetration for each blow.

3.3. Results of Variable Energy Dynamic Cone Penetrometer

In previous studies, VEDCP was performed four times on June 9, 2017 at each location (No. 1 and No. 2), and the results were reported [11]. This paper adds the results for the survey conducted at No. 1 on August 16, 2019, to the previous data. Fig. 17 shows the q_d distribution obtained from all five investigations. Each VEDCP result seems to indicate almost no change in the q_d distribution, but the result of the investigation conducted on May 5, 2016, soon after the earthquake, showed the lowest q_d distribution overall. Subsequent investigations show a tendency for q_d distribution recovery.

Figure 18(a) shows the converted N-value distribution obtained by adding existing boring data giving an initial N-value before the earthquake to the depth distribution of N-values estimated by VEDCP at position No. 1. Compared to the initial N-value, the q_d distribution 21 days after the earthquake on May 5, 2016, is clearly decreasing, but it can be seen that it closely approaches the initial N-value afterward.

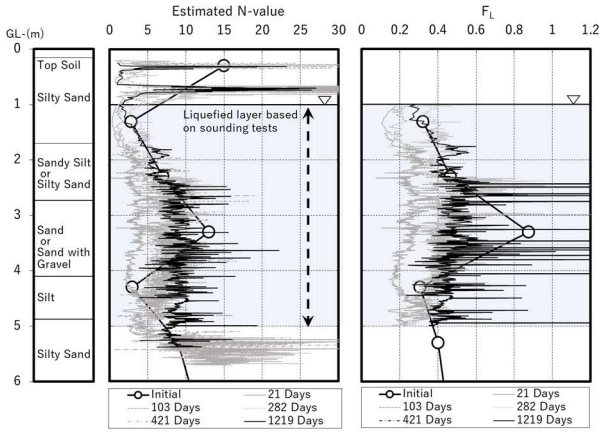

(a) N-Value (b) Liquefaction safety factor

Figure 18. Comparison before and after the 2016 Kumamoto Earthquake.

According to the depth of the initial N-value shown in Fig. 18(a), the average of the estimated N-values for each meter at GL-1.3m, -2.3m, -3.3m, and -4.3m in the liquefied layer was calculated and Fig. 19 shows these time histories. In the figure, (a) is the change in the estimated N-value; (b) is the increase in N-value, ΔN; and (c) shows the increase rate in N-value, $\Delta N/N$, with respect to the initial N-value before the earthquake. Though the plot at GL-4.3m does not show a tendency of clear decrease in N-value, a decrease in N-value and a subsequent recovery trend regardless of the depth were observed 21 days after the earthquake on May 5, 2016.

Based on these estimated N-values, Fig. 18(b) shows the F_L distribution by liquefaction susceptibility assessment assuming that the earthquake condition was Level 2 and Type II quake motion, as shown in Table 1 according to the road bridge specification [6]. This liquefaction susceptibility assessment allows interpretation of changes in ground properties, as obtained by previous studies (Section 2). Therefore, the liquefaction susceptibility assessment does not necessarily reflect the actual phenomena in the Kumamoto Earthquake. The F_L distribution 282 days after the earthquake, obtained on January 21, 2017, shows that most of the distribution has returned to the initial state before the earthquake.

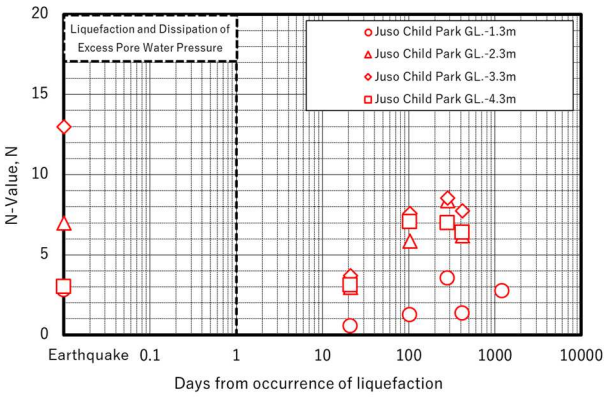

(a) Change of *N*-value in liquefied layer

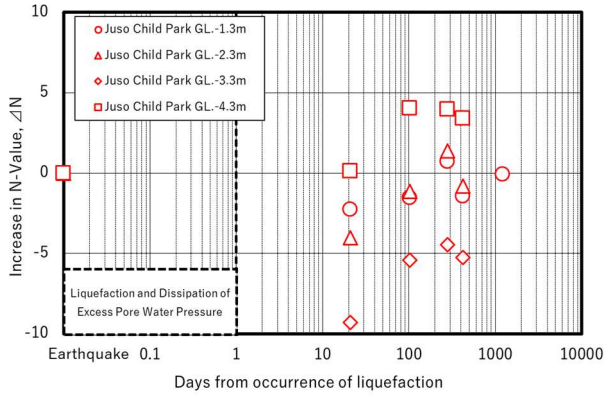

(b) Increase in *N*-value in liquefied layer

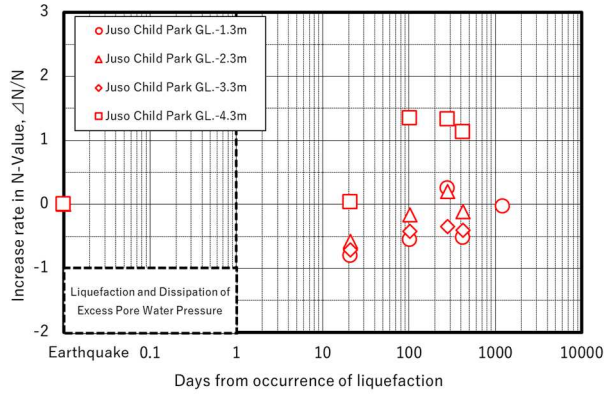

(c) Increase rate in liquefied layer

Figure 19. *N*-value trends after the 2016 Kumamoto Earthquake.

4. Consideration of recovery process of N-values after earthquakes

According to the investigation results for the 2016 Kumamoto Earthquake, the recovery tendency of *N*-values after liquefaction was not synchronized with the excess pore water pressure dissipation. In this section, to examine the long-term recovery process of *N*-values and its factors, previous investigations that could be compared with the 2016 Kumamoto Earthquake were selected. Finally, the recovery process in the liquefied layer was considered by the liquefaction potential index, P_L, as calculated from F_L.

4.1. Comparison of N-value recovery between 2016 Kumamoto and other earthquakes

The results of the Kumamoto Earthquake shown in Figs. 17 and 18 indicate that decreased *N*-values continued during the dissipation of excess pore water pressure after liquefaction, and that *N*-values began to recover later. However, because the decrease and recovery tendency of N-values differ depending on the type of ground and the liquefaction state during the earthquake, Fig. 20 shows the relationship between the initial *N*-values before an earthquake and the *N*-value change, *ΔN*, after liquefaction. In this figure, though all data are plotted, the passage of time is not considered. It is confirmed that the distribution trends of plots for each site were different. Especially, it can be seen that values at Port Island and Takenouchi Industrial Park were increasing, but values at reclaimed ground in Urayasu City were decreasing. Also, Ishikari Bay New Port and Juso Child Park have plots ranging from negative to positive, and it can be confirmed that these trends differ depending on the elapsed time.

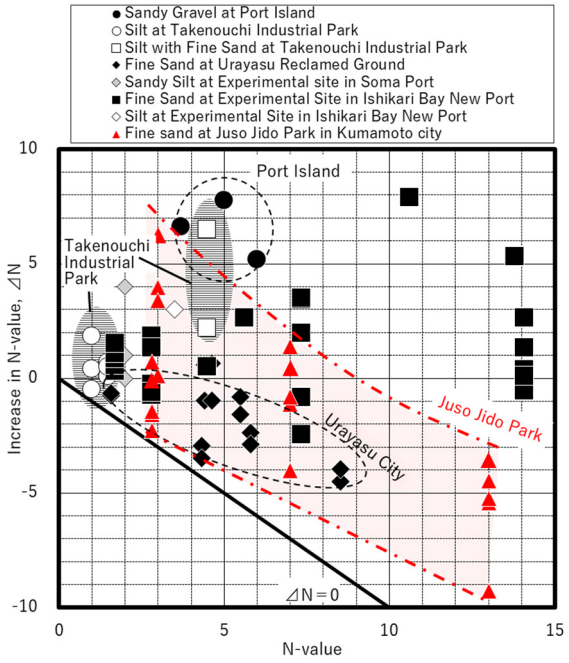

Figure 20. Summary of *N*-value changes after earthquakes.

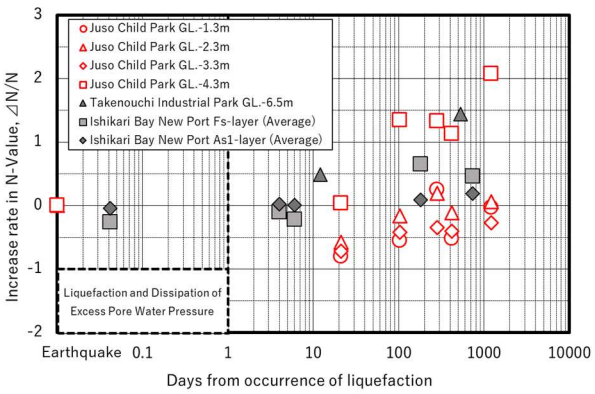

Figure 21. Time history for increase rate in *N*-values.

Based on the investigation results for Takenouchi Industrial Park, Ishikari Bay New Port, and Juso Child Park, for which enough data exist to estimate post-liquefaction

behavior, the time histories from the new investigation are added to the $\Delta N/N$ values from Fig. 19(c) in Fig. 21. After the liquefaction occurred, the N-values remained flat or decreased for about 1 month, and thereafter increased to their former level as a post-liquefaction behavior.

4.2. Effect of fine content on recovery tendency

It was confirmed that the decrease and recovery tendency of N-values after liquefaction were almost the same, but the degree of liquefaction and the timing of recovery differed. It is thought that major factors include the intensity of liquefaction and the F_c. The former can be estimated to some extent from the F_L calculated in advance, but in Figs. 3-7 and 17, there was little difference between the external force during the actual earthquake and the external force set during the F_L calculation. Therefore, because it is difficult to compare sites using F_c in the liquefied layer, the relationship between F_c and $\Delta N/N$ is shown in Fig. 22 to investigate the influence of F_c on post-liquefaction behavior. However, the reclaimed layer at Port Island consists of Masado soil with high gravel content, making it difficult to compare the effects of F_c. However, after excluding plots for Port Island, it can be confirmed that $\Delta N/N$ increases between -1 and 2 as F_c increases. In addition, Fig. 21 shows that Takenouchi Industrial Park with high F_c, Ishikari Bay New Port, and Juso Child Park had an early recovery trend except for GL-4.3m at Juso Child Park.

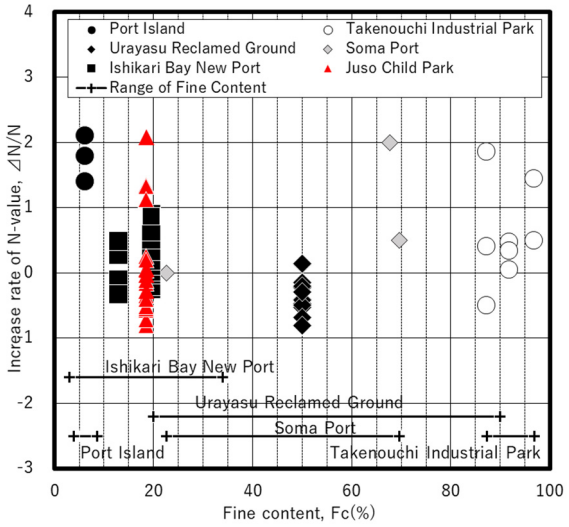

Figure 22. Relationship between fine content and increase rate of N-values.

4.3. Estimation by liquefaction potential

Based on the results of liquefaction susceptibility assessment obtained from each investigation, the liquefaction potential of the whole liquefied layer was evaluated to reveal the recovery tendency of ground properties after liquefaction. The P_L, which is an index that evaluates the liquefaction potential easily, was calculated and summarized as time histories in Fig. 23. In addition, regarding the judgment of liquefaction according to the P_L, it is evaluated as "low" at 0 to 5, "high" at 5 to 15, and "extremely high" at more than 15. P_L is expressed by the following equation using the F_L distribution [18]:

$$P_L = \int_0^{20} F \cdot W(Z)dz$$
$$F = 1 - F_L \quad (F_L \leqq 1.0)$$
$$F = 0 \quad (F_L > 1.0)$$
$$W(Z) = 10 - 0.5Z \qquad (3)$$

where $W(Z)$ is the factor according to depth and Z is the depth from the ground surface.

At Ishikari Bay New Port, the initial value of P_L was 16.2 before liquefaction, increased to 18.7 immediately after liquefaction, and returned to the initial value of 16.2 1 day after the excess pore water pressure had dissipated completely. At this stage, although the possibility of liquefaction is "extremely high", identical to the initial condition, it seems that P_L gradually decreased and the evaluation improved to a state where the possibility of liquefaction is "high". Conversely, in the case of Juso Child Park in the Kumamoto Earthquake, the initial value of P_L was 17.6 and it rose to 26.7 21 days after the earthquake. Then, the P_L showed a recovery trend and reached 18.9 after 1,219 days. At Takenouchi Industrial Park after the Tottori-ken Seibu Earthquake, 10 days after the earthquake, the initial value of P_L decreased from 14.2 to 6.1. After the 2011 Great Tohoku Earthquake, the P_L value was slightly increased 3 months after the earthquake, indicating an increased potential for liquefaction.

Based on the results of each evaluation, we focused on changes in the P_L at Ishikari Bay New Port and Juso Child Park, which have sufficient data for discussion. The former is reclaimed ground and the latter is a natural deposit. Differences at these sites suggest that the recovery behavior of ground after liquefaction depends on conditions such as sedimentation.

5. Conclusion

In this study, the results of continuous investigation of ground liquefied after the 2016 Kumamoto Earthquake were explained in detail. Also, previous severe earthquakes at locations where ground investigation was conducted at the same site before and after liquefaction were discussed. The study estimated the long-term recovery process and properties of post-liquefaction behavior from the occurrence of liquefaction to several months later.

The trends in post-liquefaction behavior obtained from changes in the estimated N-values and P_L as liquefaction potential are as follows: 1) the recovery of ground properties was not synchronized even during the process of dissipation of excess pore water pressure, 2) although there was a difference in the elapsed time after liquefaction at each site, it was confirmed that the possibility of liquefaction became lower than the initial state before the earthquake and then took a long time to recover, and 3) liquefied soil layers with higher fine content showed an earlier recovery tendency.

However, it is thought that a more detailed investigation of the m echanism is required because the amount of decrease in the N-value and its recovery tendency vary

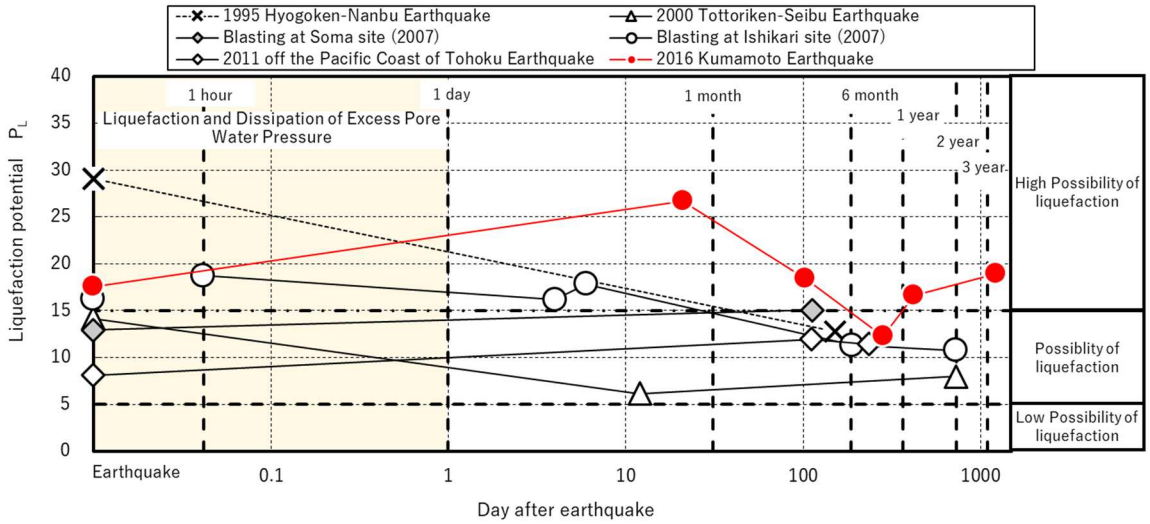

Figure 23. Changes in liquefaction potential.

depending on the ground type, degree of liquefaction, and factors such as excess pore pressure.

Acknowledgement

The authors express sincere appreciation to Mr. H. Matsuo of Eight-Japan Engineering Consultants Inc. and Ms. Y. Tadokoro of Nittoc Construction Co., Ltd. for their help in carrying out field tests at Juso Child Park after the 2016 Kumamoto Earthquake reported in the present study.

References

[1] Kazama, M., Yanagisawa, E., Inatomi, T., Sugano, T., Inagaki, H. "Stress strain relationship in the ground at Kobe island during 1995 Hyogo-ken Nanbu Earthquake inferred from strong motion array records", Journal of Japan Society of Civil Engineers, No. 547(III-36), pp. 171-182, 1996. (in Japanese) https://doi.org/10.2208/jscej.1996.547_171

[2] Japan Society of Civil Engineers "Tottori-ken Seibu Earthquake Survey Team, October 6, 2000 Tottori-ken Seibu Earthquake Survey Report", [online] Available at: https://www.jsce.or.jp/report/09/01/report.pdf [Accessed: 30 Aug. 2000].

[3] Urayasu City Liquefaction Countermeasures Study Committee "Appendix 2-4-1 Understanding of ground characteristics and liquefaction factor analysis", [online] Available at: http://www.city.urayasu.chiba.jp/menu11324.html [Accessed: 6 Sep. 2018].

[4] Nakazawa, H., Hara, T., Suetsugu, D., Kitazawa, M., Takezawa, K., Tadokoro, Y. "Ground investigation on long-term changes in soil properties after liquefaction due to the Kumamoto earthquake", Annual meeting of Japan Association for Earthquake Engineering, Tokyo, Japan, 13 Nov. 2017.

[5] Nakazawa, H., Sugano, T., Kiku, Maeda, S. "Field investigation on densification and recovery of N-value of artificial liquefied ground by controlled blast technique", Journal of Japan Society of Civil Engineers (C), 67(4), pp. 422-440, 2011. (in Japanese) https://doi.org/10.2208/jscejge.67.422

[6] Japan Road Association "Chapter 8 Influence of ground that becomes unstable during an earthquake", Specifications for Highway Bridges V, Earthquake Resistant Design, pp. 119-113, 2002. (in Japanese)

[7] Kobe city "Report on ground deformation survey of landfill site in Port Island and Rokko Island due to the Hyogo-ken Nanbu Earthquake", Kobe City, Japan, Development Department of Kobe City, 1995. (in Japanese)

[8] Tsurumi, T., Nakazawa, H., Mizumoto, K., Watanabe, H. "Post-liquefaction process based on the sedimentation of sand particles", Journal of Japan Society of Civil Engineers, No. 743(III-64), pp. 35-45, 2003. (in Japanese) https://doi.org/10.2208/jscej.2003.743_35

[9] Yamamoto, Y., Morimoto, I., Kamei, M, Yasuda, S. "Liquefaction of reclaimed deposits during Tottori-ken Seibu earthquake", In: Proceedings of the 36th Japan National Conference on Geotechnical Engineering, pp. 393-394, 2001.

[10] Nakazawa, H., Ishihara, K., Tsukamoto, Y., Kamata, T. "Investigation of in-situ elastic wave velocity for assessment of liquefaction", Journal of Japan Society of Civil Engineers (C), 62(2), pp. 346-359, 2006. (in Japanese) https://doi.org/10.2208/jscejc.62.346

[11] Ishii, C., Sasaki, S. "Change of the ground strength by the chronological order before and after the earthquake disaster judging from Swedish weight sounding test data", In: Proceedings of the 47th Japan National Conference on Geotechnical Engineering, pp. 1-2, 2012. (in Japanese)

[12] Inada, M. "Utilization for results of Swedish Weight Sounding Test", Tsuchi-to-Kiso, 8(1), pp.12-18, 1960. (in Japanese)

[13] Kusunoki, K., Nakazawa, H., Sugano, T., Okubo, Y., Kiku, H., Fujita, D. "Laboratory experiment on long-term recovery of liquefied ground state", Journal of Japan Society of Civil Engineers (A1), 69(4), pp. I_326-336, 2013. (in Japanese) https://doi.org/10.2208/jscejseee.69.I_326

[14] The 2016 Kumamoto Earthquake Ground Disaster Investigation Team "The Geotechnical Society 2016 Kumamoto Earthquake Disaster Report (Preliminary Report)", The Japanese Geotechnical Society, [online] Available at: https://www.jiban.or.jp/images/somufile/H28kumamoto_%20jishin-saigai_sokuho20160418-3.pdf [Accessed: 23 Sep. 2019). (in Japanese].

[15] Hara, T., Nakazawa, H., Tadokoro, Y., Takezawa, K., Nakane, H. "Characteristics on liquefied ground damaged by the 2016 Kumamoto earthquake", Annual meeting of Japan Association for Earthquake Engineering, Kochi, Japan, 26, Sep. 2016. (in Japanese)

[16] Public Works Research Institute "KuniJiban", [online] Available at: http://www.kunijiban.pwri.go.jp/jp/index.html [Accessed: 16 May 2016].

[17] Langton, D. D. "The Panda lightweight penetrometer for soil investigation and monitoring material compaction", Ground Engineering, pp. 33-34, Sep. 1999.

[18] Iwasaki, T., Tatsuoka, F., Tokida, K., Yasuda, S. "A practical method for assessing soil liquefaction potential based on case studies at various sites in Japan", Proceedings of 5th Japan Earthquake Engineering Symposium, pp. 641-648, 1978. (in Japanese)